



Cite this: RSC Adv., 2023, 13, 3079

 Received 28th November 2022  
 Accepted 15th January 2023

DOI: 10.1039/d2ra07575j

rsc.li/rsc-advances

## Impact of aza-substitutions on the preference of helix handedness for $\beta$ -peptide oligomers: a DFT study<sup>†</sup>

 Hae Sook Park<sup>a</sup> and Young Kee Kang<sup>ab</sup>

We studied the helix preference of the heterochiral pentamers of *cis*-2-aminocyclohexanecarboxylic acid (*c*-ACHC) and *cis*-2-aminocyclopentanecarboxylic acid (*c*-ACPC) with alternating backbone configurations by replacing  $C^{\beta}$ -aza- or  $C^{\alpha}$ -aza-peptide residues using DFT methods in solution. The helix-handedness preferences of two pentamers were strongly affected by the replacement positions (*i.e.*, chiralities) but not depending on the solvent polarity.

Azapeptides are peptide analogues in which the  $CH^{\alpha}$  or  $CH^{\beta}$  groups of the backbone of  $\alpha$ - or  $\beta$ -amino acid residues were replaced by a nitrogen atom. There have been considerable attempts in syntheses and applications of azapeptides to improve biological potencies.<sup>1–5</sup> Two kinds of  $\beta$ -peptide analogues can be generated by the aza-replacement in the  $CH^{\beta}$  or  $CH^{\alpha}$  groups of the backbone, which are  $C^{\beta}$ -aza-peptide (3-aza-

$\beta^2$ -peptide or  $\alpha$ - $N^{\alpha}$ -hydrazino) or  $C^{\alpha}$ -aza-peptide (2-aza-  $\beta^3$ -peptide or ureidopeptide) residues, respectively (Fig. 1).<sup>6,7</sup>

In particular, the isosteric substitution of the aza group in the backbone is known to affect the type and strength of H-bonds in helical foldamers of  $\beta$ -peptides.<sup>6–13</sup> Homochiral oligomers of *trans*-2-aminocyclobutanecarboxylic acid (*t*-ACBC) adopted a left-handed (*M*)-12-helix conformation both in solution and in the solid state.<sup>8</sup> However, the preferred conformation of oligomers of *t*-ACBC was switched into the (*M*)-8-helix structure, when one or two *t*-ACBC residues were replaced by the aza-substituted *t*-ACBC at the  $CH^{\alpha}$  group [*i.e.*,  $N$ -aminoazetidine-2-carboxylic acid (AAzC) residue] not depending on the position.<sup>9–11</sup>

In the case of heterochiral oligomers of *cis*-2-aminocyclopentanecarboxylic acid (*c*-ACPC) with alternating backbone configurations, *i.e.*,  $H-[ (1S,2R)-ACPC-(1R,2S)-ACPC ]_3-NH_2$ , the dominant conformation was a right-handed (*P*)-H10/12 helix in  $CD_3OH$ ,  $DMSO-d_6$ , and water.<sup>12</sup> However, the oligomer with same configurations was switched into a left-handed (*M*)-H12/10 helix by replacing the (*1R,2S*)-ACPC residue with the 2-aza-ACPC residue (*i.e.*,  $C^{\beta}$ -aza-peptide) at every even positions in the same solvents.<sup>13</sup>

We studied the helix preference of the heterochiral pentamer of *cis*-2-aminocyclohexanecarboxylic acid (*c*-ACHC) with alternating backbone configurations, *i.e.*,  $tBuO-(1S,2R)-ACHC-[ (1R,2S)-ACHC-(1S,2R)-ACHC ]_2-NHMe$ , in solution.<sup>14</sup> The dominant conformation was a left-handed (*M*)-H12/10 helix in solution but the population of the right-handed (*P*)-H10/12 helix somewhat increased as the increase of solvent polarity.

However, no report is available to study the helix preference of (i) heterochiral oligomers of *c*-ACHC by replacing  $C^{\beta}$ -aza- or  $C^{\alpha}$ -aza-peptide residues and (ii) heterochiral oligomers of *c*-ACPC by replacing  $C^{\alpha}$ -aza-peptide residue. Here, we studied the helix preference of the heterochiral pentamers of *c*-ACHC and *c*-ACPC with alternating backbone configurations by replacing  $C^{\beta}$ -

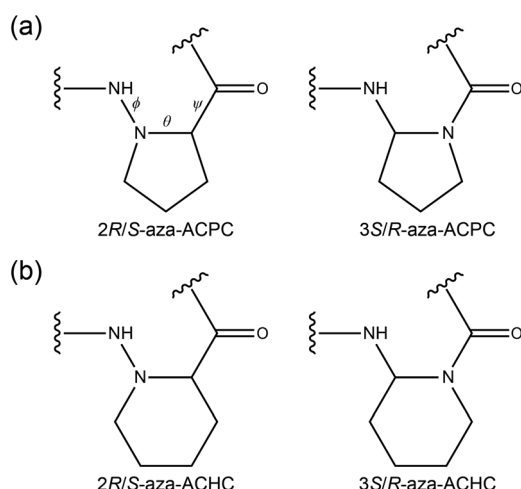


Fig. 1 Chemical structures of aza- $\beta$ -peptide residues: (a)  $C^{\beta}$ -aza-(left) and  $C^{\alpha}$ -aza-peptide (right) residues of *cis*-ACPC and (b)  $C^{\beta}$ -aza-(left) and  $C^{\alpha}$ -aza-peptide (right) residues of *cis*-ACHC.

<sup>a</sup>Department of Nursing, Cheju Halla University, Cheju 63092, Republic of Korea

<sup>b</sup>Department of Chemistry, Chungbuk National University, Cheongju, Chungbuk 28644, Republic of Korea. E-mail: ykkang@chungbuk.ac.kr

† Electronic supplementary information (ESI) available. See DOI: <https://doi.org/10.1039/d2ra07575j>



aza- or C<sup>α</sup>-aza-peptide residues (Fig. 1) depending on the position and solvent polarity using DFT methods in solution.

In this work, the helix preference was investigated for two heterochiral pentamers of *c*-ACHC and *c*-ACPC with alternating backbone configurations, *i.e.*, Ac-(1*S*,2*R*)-ACHC-[(1*R*,2*S*)-ACHC-(1*S*,2*R*)-ACHC]<sub>2</sub>-NHMe (**1**) and Ac-(1*S*,2*R*)-ACPC-[(1*R*,2*S*)-ACPC-(1*S*,2*R*)-ACPC]<sub>2</sub>-NHMe (**2**).

All DFT calculations were performed using the M06-2X,<sup>15</sup> functional implemented in the Gaussian 09 program.<sup>16</sup> The geometry optimizations were carried out at the M06-2X/6-31+G(d) level of theory and followed by single-point energy ( $E_{sp}$ ) calculations at the M06-2X/def2-TZVP level of theory. The M06-2X/6-31+G(d) level of theory exhibited good performance against the observed rotational constants of the most stable conformer of Ac-Ala-NHMe with RMSD = 0.9 MHz.<sup>17</sup> The M06-2X/def2-TZVP//M06-2X/6-31+G(d) level of theory well reproduced the relative CCSD(T)/CBS-limit energies of local minima of Ac-Ala-NHMe and Ac-Pro-NHMe (ref. 17) with RMSD = 0.10 and 0.08 kcal mol<sup>-1</sup>, respectively. The solvation free energies ( $\Delta G_s$ ) were calculated at the M06-2X/6-311G(d,p) level of theory using the implicit PCM<sup>18</sup> solvation method in chloroform, acetonitrile, DMSO, and water. The population of each helix was estimated using the relative energy ( $\Delta E_s$ ) obtained by the sum of  $\Delta E_{sp}$  and  $\Delta \Delta G_s$  at 25 °C in solution. Recently, the M06-2X/def2-TZVP//M06-2X/6-31+G(d) level of theory with the PCM method appeared to be appropriate in predicting the conformational preferences and the *cis-trans* isomerization of the longer peptides containing Pro or Pro derivatives in chloroform.<sup>19</sup>

The structures of (*M*)- and (*P*)-helices of *cis*-ACHC pentamer **1** optimized at the M06-2X/6-31G(d) level of theory<sup>14</sup> were used to generate the initial structures of *cis*-ACPC pentamer **2** and the corresponding both pentamer analogues containing aza-residues. Aza-containing analogues of pentamers **1** and **2** considered here were constructed by aza-substitutions only at even or odd positions to investigate the positional dependence. This is because the residues at even or odd positions have the same chiralities. GaussView<sup>20</sup> was used in constructing the initial structures for optimization. All helices of pentamer **1** and **2** and their aza-analogues were reoptimized at the M06-2X/6-31+G(d) level of theory.

The optimized structures of *c*-ACHC pentamer **1** and *c*-ACPC pentamer **2** are shown in Fig. 2. In the (*M*)-H12/10 helix of pentamer **1**, there were two  $C_{12}$  H-bonds between  $C=O$  (*i* - 1) and  $H-N$  (*i* + 2) with the distances 2.94 and 2.90 Å; and two  $C_{10}$  H-bonds between  $H-N$  (*i*) and  $O=C$  (*i* + 1) with the distances 2.97 and 2.98 Å. The (*P*)-H10/12 helix of pentamer **1** also had two  $C_{10}$  H-bonds with the distances 2.90 and 2.93 Å; and two  $C_{12}$  H-bonds with the distances 2.93 and 2.90 Å. The  $C_{10}$  H-bonds were somewhat shorter in the (*P*)-helix than those in the (*M*)-helix. In both (*M*)- and (*P*)-helices of pentamer **2**, the types of H-bonds were quite similar to those of pentamer **1**. However, both  $C_{12}$  and  $C_{10}$  H-bonds became about 0.05 Å shorter in pentamer **2** than those in pentamer **1**. Because the types and distances of H-bonds were similar in both (*M*)- and (*P*)-helices of aza-substituted pentamers **1** and **2**, no further comparison was made in detail. The optimized structures of (*M*)- and (*P*)-helices of both pentamer analogues containing aza-residues are shown

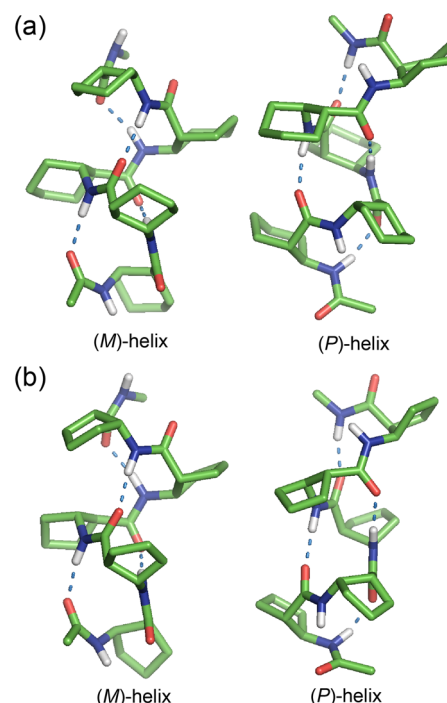


Fig. 2 The structures of (*M*)- and (*P*)-helices of (a) *cis*-ACHC pentamer **1** and (b) *cis*-ACPC pentamer **2** optimized at the M06-2X/6-31+G(d) level of theory. For clarity, all non-polar hydrogen atoms are omitted. All H-bonds are represented by dotted lines.

in Fig. S1–S4 of ESI.† The corresponding relative conformational energies, and relative solvation free energies, and absolute electronic energies are shown in Tables S1 and S2 of ESI.† The Cartesian coordinates of all optimized structures are also listed in ESI.†

The relative populations of (*M*)- and (*P*)-helices for *c*-ACHC pentamer **1** and their aza-substituted analogues were shown in Fig. 3. The relative populations of (*M*)- and (*P*)-helices for pentamers **1** (shown in the first column of each set of histograms in Fig. 3a and b) were calculated as 80 : 20 and 67 : 33 in chloroform and acetonitrile, respectively, which are consistent with the observed values of 80 : 20 and 63 : 37, respectively.<sup>14</sup> There was somewhat the increase of the population of the right-handed (*P*)-helix as the increase of solvent polarity. However, there were dramatic shifts from (*P*)-helix to (*M*)-helix for pentamer **1** when either even or odd residues with (1*R*,2*S*) or (1*S*,2*R*) configurations, respectively, were replaced by C<sup>β</sup>-aza residues in all four solvents. However, the replacements by C<sup>α</sup>-aza residues at even or odd positions resulted in only (*P*)- or (*M*)-helix, respectively in all solvents.

Fig. 4 depicted the relative populations of (*M*)- and (*P*)-helices for *c*-ACPC pentamer **2** and their aza-substituted analogues. The (*P*)-H10/12 helix of pentamer **2** was preferred by 73 : 27 (shown in the first column of each set of histograms in Fig. 4a and b), which is consistent with the experimental results in CD<sub>3</sub>OH, DMSO-*d*<sub>6</sub>, and water,<sup>12</sup> its population was somewhat increased in acetonitrile, DMSO, and water (Fig. 4). The dramatic shifts of (*P*)-helix to (*M*)-helix were found for pentamer **2** when even



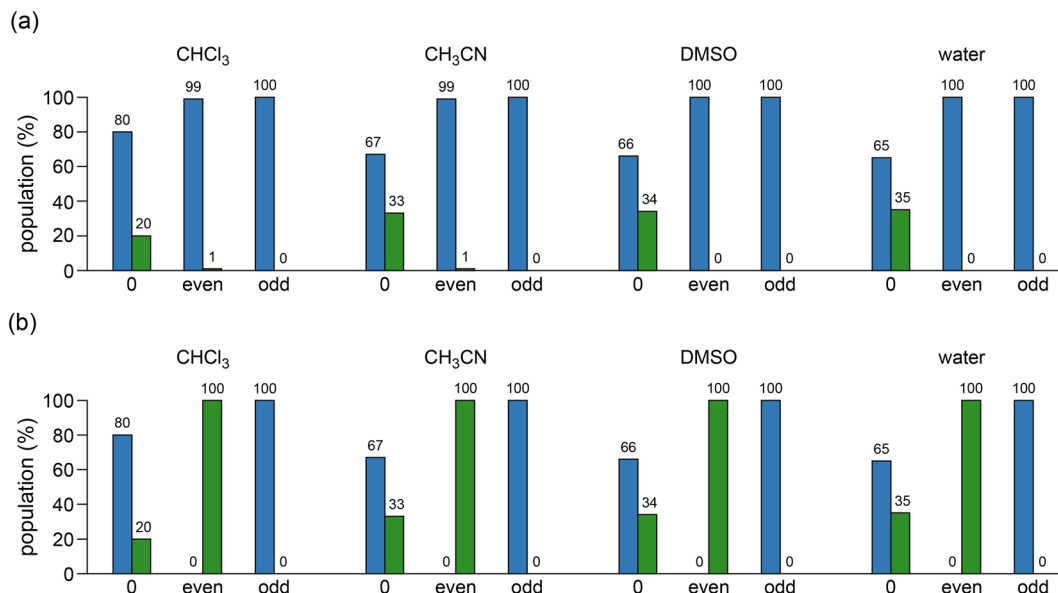


**Fig. 3** The populations of (*M*)- and (*P*)-helices for *cis*-ACHC pentamer **1** in chloroform, acetonitrile, DMSO, and water by the replacements of (a) C<sup>β</sup>-aza and (b) C<sup>α</sup>-aza residues. The blue and green histograms correspond to the populations of (*M*)- and (*P*)-helices, respectively. The types of replacements of "no replacement", "replacement at even residues", and "replacement at odd residues" are represented as "0", "even", and "odd" on the horizontal axis, respectively.

residues were replaced by C<sup>β</sup>-aza residues in all four solvents, whereas the replacements at odd residues retained the preference of the (*P*)-helix in acetonitrile, DMSO, and water but some decrease in its population in chloroform. However, the replacements by C<sup>α</sup>-aza residues at even or odd positions for pentamer **2** resulted in only (*P*)- or (*M*)-helix, respectively in all solvents, as the same as for pentamer **1**.

In summary, the replacement of C<sup>β</sup>-aza residues brought *cis*-ACHC pentamer **1** to only the (*M*)-helix not depending on the position (*i.e.*, chirality) and the solvent polarity, whereas the helix-handedness preference of *cis*-ACPC pentamer **2** was affected by the replacements at even or odd positions independent of the solvent polarity. However, the replacements by C<sup>α</sup>-aza residues at even positions or odd positions resulted in only (*P*)- or (*M*)-

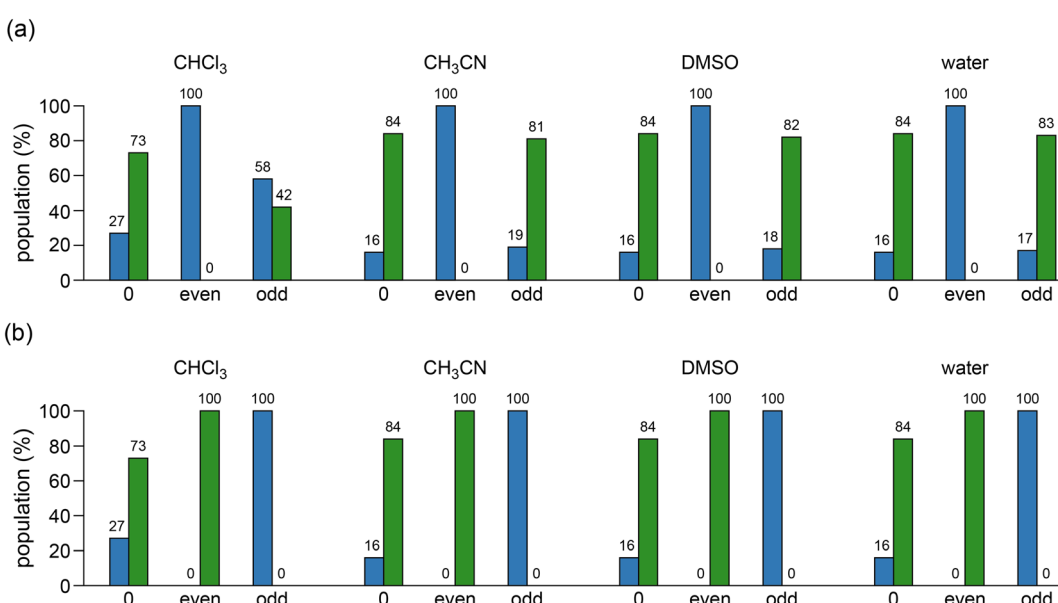


**Fig. 4** The populations of (*M*)- and (*P*)-helices for *cis*-ACPC pentamer **2** in chloroform, acetonitrile, DMSO, and water by the replacements of (a) C<sup>β</sup>-aza and (b) C<sup>α</sup>-aza residues. The blue and green histograms correspond to the populations of (*M*)- and (*P*)-helices, respectively. The types of replacements of "no replacement", "replacement at even residues", and "replacement at odd residues" are represented as "0", "even", and "odd" on the horizontal axis, respectively.



helix, respectively, for both pentamers **1** and **2** not depending on the solvent polarity. Hence, the results obtained in this work would provide useful structural information for the design of bioactive helical  $\beta$ -peptides with either left- or right-handedness.

## Conflicts of interest

There are no conflicts to declare.

## Acknowledgements

This research was supported by Basic Science Research Program through the National Research Foundation of Korea (NRF) funded by the Ministry of Education (2020R1I1A3053400).

## References

- 1 T. A. Martinek and F. Fülöp, *Chem. Soc. Rev.*, 2012, **41**, 687.
- 2 I. Avan, C. D. Hall and A. R. Katritzky, *Chem. Soc. Rev.*, 2014, **43**, 3575.
- 3 R. Chingle, C. Proulx and W. D. Lubell, *Acc. Chem. Res.*, 2017, **50**, 1541.
- 4 A. Begum, D. Sujatha, K. V. S. R. G. Prasad and K. Bharathi, *Asian J. Chem.*, 2017, **29**, 1879.
- 5 K. Tarchoun, M. Yousef and Z. Bánóczi, *Future Pharm.*, 2022, **2**, 293.
- 6 L. Fischer, C. Didierjean, F. Jolibois, V. Semetey, J. M. Lozano, J.-P. Briand, M. Marraud, R. Poteau and G. Guichard, *Org. Biomol. Chem.*, 2008, **6**, 2596.
- 7 R.-O. Moussodia, E. Romero, E. Wenger, B. Jamart-Grégoire and S. Acherar, *J. Org. Chem.*, 2017, **82**, 9937.
- 8 C. Fernandes, S. Faure, E. Pereira, V. Théry, V. Declerck, R. Guillot and D. J. Aitken, *Org. Lett.*, 2010, **12**, 3606.
- 9 A. Altmayer-Henzién, V. Declerck, J. Farjon, D. Merlet, R. Guillot and D. J. Aitken, *Angew. Chem., Int. Ed.*, 2015, **54**, 10807.
- 10 V. Declerck and D. J. Aitken, *J. Org. Chem.*, 2018, **83**, 8793.
- 11 Z. Imani, R. Guillot, V. Declerck and D. J. Aitken, *J. Org. Chem.*, 2020, **85**, 6165.
- 12 T. A. Martinek, I. M. Mándity, L. Fülöp, G. K. Tóth, E. Vass, M. Hollósi, E. Forró and F. Fülöp, *J. Am. Chem. Soc.*, 2006, **128**, 13539.
- 13 A. Hetényi, G. K. Tóth, C. Somlai, E. Vass, T. A. Martinek and F. Fülöp, *Chem.-Eur. J.*, 2009, **15**, 10736.
- 14 S. Shin, M. Lee, I. A. Guzei, Y. K. Kang and S. H. Choi, *J. Am. Chem. Soc.*, 2016, **138**, 13390.
- 15 Y. Zhao and D. G. Truhlar, *Theor. Chem. Acc.*, 2008, **120**, 215.
- 16 M. J. Frisch, G. W. Trucks, H. B. Schlegel, G. E. Scuseria, M. A. Robb, J. R. Cheeseman, G. Scalmani, V. Barone, B. Mennucci, G. A. Petersson, H. Nakatsuji, M. Caricato, X. Li, H. P. Hratchian, A. F. Izmaylov, J. Bloino, G. Zheng, J. L. Sonnenberg, M. Hada, M. Ehara, K. Toyota, R. Fukuda, J. Hasegawa, M. Ishida, T. Nakajima, Y. Honda, O. Kitao, H. Nakai, T. Vreven, J. A. Montgomery Jr, J. E. Peralta, F. Ogliaro, M. Bearpark, J. J. Heyd, E. Brothers, K. N. Kudin, V. N. Staroverov, R. Kobayashi, J. Normand, K. Raghavachari, A. Rendell, J. C. Burant, S. S. Iyengar, J. Tomasi, M. Cossi, N. Rega, J. M. Millam, M. Klene, J. E. Knox, J. B. Cross, V. Bakken, C. Adamo, J. Jaramillo, R. Gomperts, R. E. Stratmann, O. Yazayev, A. J. Austin, R. Cammi, C. Pomelli, J. W. Ochterski, R. L. Martin, K. Morokuma, V. G. Zakrzewski, G. A. Voth, P. Salvador, J. J. Dannenberg, S. Dapprich, A. D. Daniels, Ö. Farkas, J. B. Foresman, J. V. Ortiz, J. Cioslowski and D. J. Fox, *Gaussian 09 (Revision D.01)*, Gaussian, Inc., Wallingford, CT, 2013.
- 17 H. S. Park and Y. K. Kang, *Chem. Phys. Lett.*, 2014, **600**, 112.
- 18 B. Mennucci, R. Cammi and J. Tomasi, *J. Chem. Phys.*, 1999, **110**, 6858.
- 19 H. S. Park and Y. K. Kang, *New J. Chem.*, 2019, **43**, 17159.
- 20 R. D. Dennington II, T. A. Keith and J. Millam, *GaussView (Version 6.0)*, Gaussian, Inc., Wallingford, CT, 2016.

